

Multifunctional HDO/Selective Cracking Ni/HBEA Catalysts to Produce Jet Fuel and Diesel from Bio-oils

Salvatore Abate*, Gianfranco Giorgianni, Paola Lanzafame, Siglinda Perathoner, Gabriele Centi

University of Messina, Section Industrial Chemistry, INSTM/CASPE (Laboratory of Catalysis for Sustainable Production and Energy) and ERIC aisbl (European Research Institute of Catalysis), V.le F. Stagno D'Alcontres 31, 98166 Messina (Italy)
 abates@unime.it

The development of multifunctional catalysts to selectively produce in one-step processes jet fuels (around C12) and diesel (around C16-C18) from bio-oils (vegetable and especially algal oil) is still a challenge to produce next-generation biofuels. This topic is addressed here by investigating the activity of Ni based catalysts in the methyl palmitate conversion, as model test reaction. The performance of Ni/HBEA (8%wt Ni) catalysts, where mesoporosity was introduced by desilication, were compared with those of mesoporous SBA-15. It is evidenced that desilication allows to introduce selective hydrocracking functionality together with HDO (hydrodeoxygenation), the latter prevailing occurring through hydrogenation of the acid group rather than via hydrodecarboxylation.

1. Introduction

Catalysis has a pivotal role in many of the critical refinery processes, but the introduction of biofuels poses new problems and needs, particularly to develop 2nd and especially 3rd generation catalytic processes (Abate et al., 2015). Algal oil is one of the raw materials for 3rd generation processes (Yusuf, 2013) but in addition to the issues related to its recovery from microalgae and cost of production, the downstream processing require still improvements. Current studies are focused mainly on production of biodiesel by transesterification (Park et al., 2015). The main drawback of this technology are: i) the high costs of algal oil purification, ii) the coproduction of glycerol, and the need of methanol co-feeding, and iii) the low yields in more valuable jet fuels cut. UOP/ENI and Neste Oil processes are the two better-known 2nd generation technologies for the production of bio jet-fuel from vegetable oils (Wang et al., 2016). After the hydrodeoxygenation of triglycerides (HDO), an additional isomerization/cracking stage is required (Baldiraghi et al., 2009; Wang et al., 2016). Current results based on the use of vegetable oils rather than algal oil, report a broad range of products, going from gasoline to diesel. It is thus valuable to look at the possibility of one stage process, which can furthermore maximize the jet fuel cut.

Recently, catalysts based on Ni/zeolite to synthesize green diesel from lipid fractions of microalgae have been developed (Peng et al., 2012; Zhao et al., 2013). The possibility to produce jet fuels range in a single step process over Ni-W/ZSM-5 or sulfided Ni-Mo/HZSM5 catalysts with hierarchical structure has been reported by Verma et al. (2011), but not further studied later. In addition, quite severe reactions conditions were required. The hydroconversion of Jatropha Oil over hierarchical ZSM-5 was studied by Chen et al. (2014), reporting that mesoporosity improves the selectivity to jet fuels cut. These catalysts reject oxygen only by decarboxylation, being missing the hydrogenation function. It is thus interesting to study hierarchical-type Ni/zeolite, particularly the beta-type (BEA) being the more active in algal oil conversion, to evaluate their use as multi-functional catalyst able to combine hydrodeoxygenation (HDO) to selective cracking (to jet cut) functions.

2. Experimental

2.1 Preparation of the Catalysts

Two commercial BEA zeolites supplied by Zeolyst (CP811E-75, CP814E) and a home-made mesoporous

silica (SBA-15) were used. The CP811E-75D zeolite was obtained by a standard desilication procedure (Verboekend et al., 2011), starting from the zeolites CP811E-75. After the desilication stage, the CP811E-75D was exchanged by a NH_4NO_3 solution, dried at 110°C and calcined (450°C , 6h, $2^\circ\text{C}/\text{min}$) to obtain the protonic form. 8%wt Ni was deposited by incipient wetness method (Peng et al., 2012) by using $\text{Ni}(\text{NO}_3)_2 \cdot 6\text{H}_2\text{O}$ as the precursor. Ni was introduced on calcined CP814E with the same procedure. The catalysts were then dried overnight at room temperature, then at 110°C for 12h, and finally calcined at 400°C for 4h with a heating rate of $2^\circ\text{C}/\text{min}$. The calcined catalysts were reduced, before each test, in a tubular reactor using a flow of H_2 (100ml/min, 500°C , $2^\circ\text{C}/\text{min}$, 4h). The SBA-15 was prepared as earlier reported (Abate, et al., 2011) and reduced as described above.

2.2 Characterization

The porosity and surface area were determined by N_2 physisorption at 77K (Micromeritics ASAP2010). The micropore volume (V_μ) and mesoporous surface area (S_{meso}) were determined by t-plot method. Mesoporous volume was calculated by subtracting the microporous volume from the total pore volume. The Hierarchy Factor (Pérez-Ramírez et al., 2009) was used to characterize the hierarchy of the zeolites. The structure of the catalysts was analysed by XRD (Bruker D2 Phaser). The nickel crystallite size was determined by the Scherrer equation, by using the (111) and the (200) reflection shown at 2θ , 44.425° and 51.765° . The acidity of the zeolites was characterized by NH_3 Temperature Programmed Desorption (TPDA). TPDA measurements in the range $150\text{--}700^\circ\text{C}$ were performed in a U-quartz reactor containing about 100 mg of the sample. The reactor was fed by using a mixture 5% H_2/Ar for 4h at 500°C . NH_3 was adsorbed at 150°C for 1h by using a mixture 10% NH_3/He , followed by purging in He flow for 90 min. Blank tests were made to consider dehydroxylation of the support and baseline shifts (Costa et al., 2000). The metal surface area was analysed by pulse CO chemisorption (stoichiometry factor $\text{CO}/\text{Ni}=1$). TPDA and CO chemisorption analysis were made by using Micromeritics Autochem II apparatus. TEM analysis was made with a PHILIPS CM12 Microscope equipped with EDX (Phenom ProX).

2.3 Testing

The catalysts were tested in a batch reactor at 240°C and 40 barg, by using a 300ml Parr Autoclave for a reaction time of 4h. The tests were conducted in 100ml of n-heptane as solvent and by using Methyl Palmitate (MP) as model compound (1g/100ml) with a catalyst concentration of 0.1g/100ml. The reaction was started by opening the catalyst addition device by a little H_2 overpressure. Liquid samples were taken from the reactor at the beginning, after 2h and at the end of the reaction (4h) and analyzed by GC/MS and GC-FID by using a Restek Rxi-5MS column.

3. Results and discussion

3.1 Characterization

The Si/Al ratio of CP814E and CP811E-75 samples are respectively 12.5 and 37.5, respectively. Table 1 reports the textural features of the samples. CP814E and CP811E-75 zeolites have quite similar characteristics. The desilicated zeolite CP811E-75D, with respect to the parent zeolite, shows an increase in the BET surface area in the mesopore region at the expense of the micropore volume and micropore surface area, in line with literature data for the desilication treatment (Pérez-Ramírez et al., 2009). The XRD profiles reported in Figure 1 – XRD profiles for all the supports investigated evidence the typical reflections of BEA structure for the parent zeolites, with a loss of crystallinity for the desilicated sample.

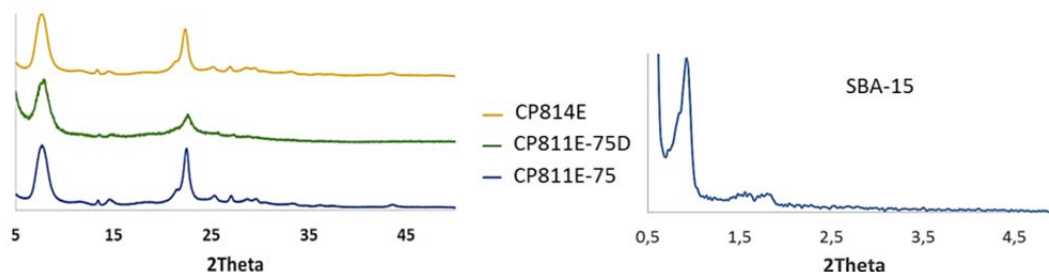


Figure 1 – XRD profiles for all the supports investigated

TEM micrographs (Figure 2) of Ni/CP814E reveal the presence of small Ni particles, while bigger particles are present in Ni/CP811E-75 and Ni/CP811E-75D. The results of CO pulse chemisorption are reported in Table 2. The higher dispersion of Ni in CP814E is likely related to higher hydrophilicity (lower Si/Al ratio), which allow a

better wetting by the impregnating solution. This is the reason of the lower size of Ni particle in Ni/CP814E with respect to other samples. It should be noted that the size of Ni particles is determined by elaboration of data of CO chemisorption, while TEM data show the presence of smaller particles. Nevertheless, data evidence that in Ni/CP811E-75 samples (before and after desilication) and in Ni/SBA-15 sample, large Ni particles, located out of the zeolite micropores, are predominantly present. The crystallite size of Ni, measured by using the Scherrer equation, is also shown in Table 2. The discordances between CO chemisorption and XRD data on the average size of Ni particles is likely due to the quite large distribution in sizes observed for Ni/CP811E-75 samples (before, after desilication) and Ni/SBA-15.

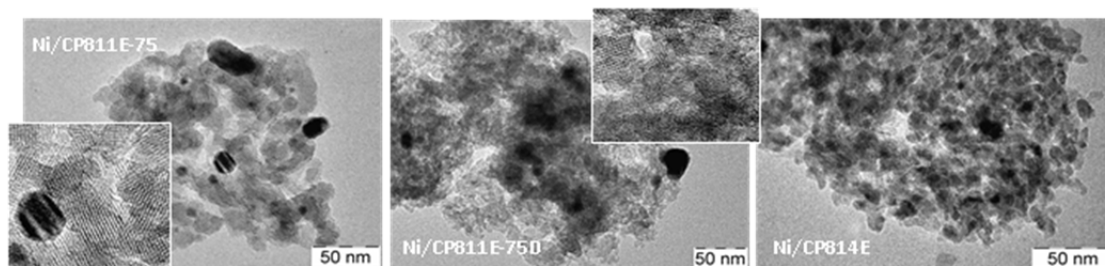


Figure 2 - TEM micrographs for the catalysts

Table 1 – Main textural data of the catalysts

Support	S_A BET [m^2/g]	Pore Vol. [cm^3/g]	V_μ [cm^3/g]	V_{meso} [cm^3/g]	S_μ [m^2]	S_{meso} [m^2/g]	HF
CP814E	624.22	0.97	0.17	0.80	426.23	197.99	0.056
CP811E-75	590.16	1.00	0.16	0.85	388.47	201.67	0.053
CP811E-75 D	677.91	1.09	0.07	1.03	140.15	537.75	0.047
SBA-15	189.70	0.29	0	0.29	0	189.70	n.d.

Table 2 - Ni surface area and particle size (^a determined by AAS; ^b determined by CO chemisorption; ^c Cubic crystal size; ^d determined by XRD on freshly reduced catalysts)

Prepared Catalysts	%Ni ^a	MSA [m^2/g_{Ca}] ^b	Ni Particle size[nm] ^{b,c}	Ni Crystallite size ^d
Ni/CP814E	7.87	4.72	9.4	13
Ni/CP811E-75	8.31	1.19	39	9.1
Ni/CP811E-75D	7.31	0.57	71	16.7
Ni/SBA-15	7.61	0.70	72	9.7

The TPDA profiles for the parent and desilicated zeolites are reported and Figure 3. The TPDA curves can be deconvoluted in three Gaussian shape peaks (Derouane et al., 2013; van Laak et al., 2011) and the main results are reported in Table 3. The LT peaks are generally associated with NH_3 weakly chemisorbed or physically adsorbed on weak Lewis acid sites like Na^+ (Niwa et al., 1997). The MT peak is related to the number of Al atoms in the framework, and to the Brønsted acidity of the zeolites (Miyamoto et al., 2000; van Laak et al., 2011). As expected, the area of the MT peaks gives a higher density of acid sites for CP814E ($Si/Al_{bulk}=12.5$), followed by the CP811E-75D ($Si/Al_{bulk}<37.5$) and then by the CP811E-75 ($Si/Al_{bulk}=37.5$). Moreover, the MT peak for the CP811E-75D shows a shift to lower temperatures and a higher density of acid sites (Niwa et al., 1997) than the parent zeolites, due to the lower Si/Al ratio and contribution of micropores. The latter is probably related to a decrease of the confinement effect (Hunger et al., 2002) or by the improved diffusion of ammonia because of hierarchical porosity. The HT peak was attributed to strong Lewis sites (van Laak et al., 2011). The maximum of the peak is at nearly the same temperature for all the samples, while the area depends on the zeolites. Comparing the desilicated zeolite with the parent one, the area of the HT peak is at almost three times larger for the desilicated sample, likely due to the migration of part of Al to extra-framework sites during the desilication treatment and consequent increase of Lewis acidity (Verboekend et al., 2011). The $Si/Al_{surface}$, by EDX, are 9.5, 11.3 and 22.1 for CP814E, CP811E-75D and CP811E-75 respectively.

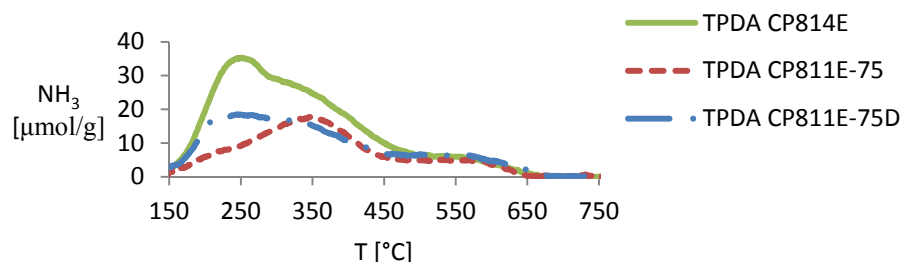


Figure 3 TPDA curves for the parent and desilicated zeolites (blank subtracted).

Table 3 – TPDA deconvolution results

Zeolite	LT [μmol/g, °C]	MT [μmol/g, °C]	HT [μmol/g, °C]	NH ₃ total [μmol/g]	NH ₃ [μmol/m ²]	NH ₃ Micropores [μmol]	NH ₃ Mesopores [μmol]
CP814E	221.3 (236.7)	492.1 (330.7)	89.9 (540.7)	783.3	0.79	336.1	156.1
CP811E-75	48.4 (216.4)	279.6 (343.3)	40.4 (543.7)	404.2	0.47	184.5	95.3
CP811E-75D	78.9 (222.9)	331.5 (316.2)	113.6 (540.4)	524	0.49	68.5	262.9

3.2 Testing

Role of the acidity

Figure 4 shows the conversion of methyl palmitate and yield to main products: palmitic acid (PA), n-hexadecane (n-C16), and n-pentadecane (n-C15). The catalysts are reported following the bulk Si/Al ratio order. Fig. 4 also shows the Ni surface area, the acidity strength and the $(\mu\text{molNH}_3/\text{g})/(\text{m}^2\text{Ni})$ ratio, the latter as a relative measure of activity vs. hydrogenation activity. Ni/SBA-15, due its low-acidity, show rather low performances. The HDO reaction thus requires an acid function together with the hydrogenation one. The best activity shown by Ni/CP811E-75 catalyst, even was expected by Ni/CP814E having higher total amount of Brønstead acid sites (lower Si/Al ratio) and smaller Ni particles, preferably localized inside the zeolite. Therefore, localization of Ni inside the zeolite, likely due to the restricted accessibility, is probably negative for the activity. However, after desilication of this sample, the activity becomes comparable to that of Ni/CP814E sample, likely in this case being desilication decreasing too much the amount of Brønstead acid sites, with part of the Al also migrating to extra-framework positions. The maximum performances thus depend on the optimal concentration of hydrogenation and acid sites, but also their accessibility. It may be also noted that C16 yield is higher than C15, the former deriving from the hydrogenation of PA, while C15 deriving from decarboxylation of PA. There is an inverse relation between PA yields and C16/C15 yields, in agreement with the idea that PA is the intermediate to C15/C16.

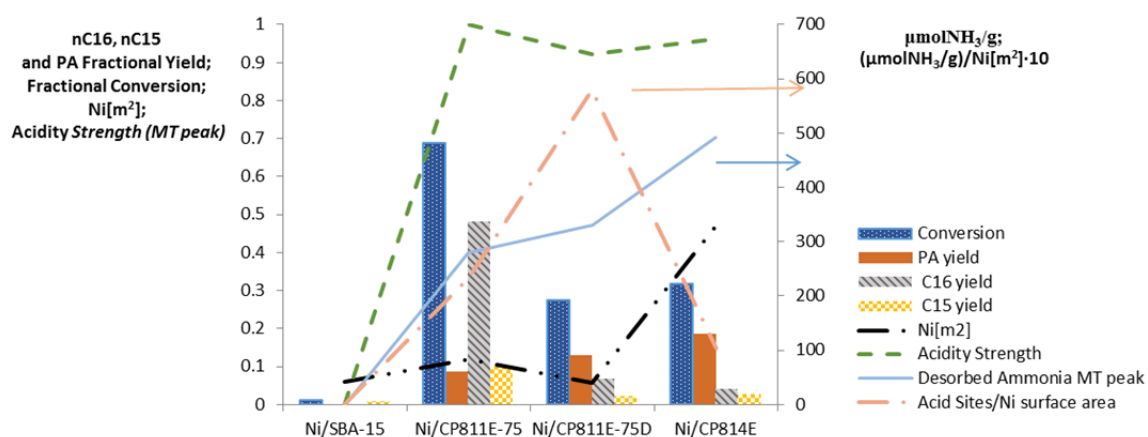


Figure 4 – Conversion and yields of the most abundant intermediates for the catalysts tested.

Effect of the mesoporosity

Figure 5 reports the analysis of the distribution of products (as a function of carbon atoms in the molecule) for the catalysts tested. In addition, small amounts of cetyl alcohol, cetyl palmitate and di-cetyl ether observed. This is consistent with the acidity of the catalysts. Furthermore, the amount of isomers, mainly i-C16 and i-C15 (not evidenced in the plots), increases with the time of reaction. The most striking result, in the comparison of Ni/CP811E-75 and Ni/CP811E-75D catalysts, is the increased amount of products in the range of C9-C12 in the latter. Although the desilicated catalyst is less active (Fig. 4), there is a selective cracking of the products to form selectively C12 products (with minor amounts of C9), especially for the shorter time of reaction, likely because these products further react. It should be noted that to obtain a C12 hydrocarbons from a C16 or C15 hydrocarbon is not an expected result from a simple statistical cracking.

We not observed significant amounts of C9-C12 products using the Ni/CP814E zeolite. This is consistent with the idea that the hydrogenation function should be located external to micropores of the zeolite, but likely in close vicinity to Lewis acid sites (related to extra-framework Al), and channels in which the hydrocarbon is partially adsorbed (pore mouth cracking mechanism, Souverijns et al., 1998). We may also note that a correlation between the HF factor (Pérez-Ramírez et al., 2009) and catalytic behavior is not observed, consistent with the above comment on the tentative mechanism.

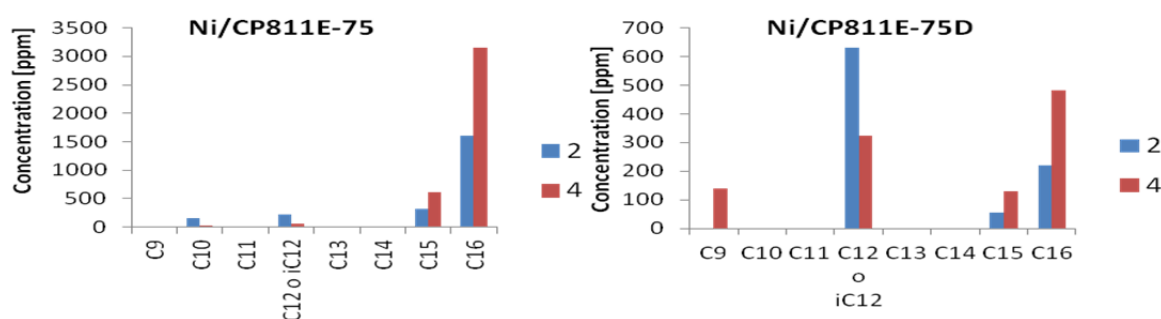


Figure 5 – Product distribution for the catalysts tested, after 2 h (blue) and 4 h (red) of reaction time

4. Conclusions

The comparison of the performances of Ni/HBEA with different Si/Al ratio (before and after desilication) and Ni/SBA-15 catalysts in the conversion of methyl palmitate, used as model molecule, to develop catalysts for the one-step combined HDO and selective cracking of algal oil, show some interesting results. Different aspects govern the reactivity in the conversion of methyl palmitate: i) the localization of Ni particles (when located inside the zeolite channels lower performances were observed), ii) the acidity of the zeolite (Brønsted acidity is necessary together with the hydrogenation function related to Ni), and iii) the presence of mesoporosity. The latter, together with the presence of extra-framework Al sites, however, is necessary to provide a mechanism of selective cracking, via likely a pore mouth reaction mechanism.

Although these data require further studies to investigate more in detail how to optimize the catalytic performances, and understand in a more detail the reaction mechanism, the results provide good indications on how to develop novel catalysts for one-step combined HDO/selective cracking of algal oil. Current data do not give indications on issues of stability, but certainly, the direct use of algal oil, and its degree of purity, may influence this aspect.

Acknowledgments

This work was realized with the financial support of the PRIN 2010-11 project “Innovative processes for the conversion of algal biomass for the production of jet fuels and green diesel” and of the project WAVES (Waste bio-feedstocks hydro-Valorization processes) financed by MIUR in the frame of ERA-NET CAPITA.

Reference

- Abate, S., Centi, G., & Perathoner, S. (2015). Energy-related catalysis. *National Science Review*, 2(2), 143–145. doi:10.1093/nsr/nwv017
- Abate, S., Lanzafame, P., Perathoner, S., & Centi, G. (2011). SBA-15 as a support for palladium in the direct synthesis of H₂O₂ from H₂ and O₂. *Catalysis Today*, 169(1), 167–174. doi:10.1016/j.cattod.2010.09.030

- Alotaibi, F. M., Abudawood, R. H., Al-Megren, H. a., Al-Kinany, M. C., Jamea, E. H., & Garforth, A. a. (2014). The catalytic stability of some selected bifunctional nanoporous-based catalysts in the hydroisomerisation of n-C7 and the effect of post-synthesis modification techniques. *Applied Petrochemical Research*, 4(1), 95–136. doi:10.1007/s13203-014-0057-y
- Baldiraghi, F., Stanislao, M. Di, Faraci, G., Perego, C., Marker, T., Gosling, C., Kokayeff, P., Kalnes, T., Marinangeli, R. (2009). Ecofining: New Process for Green Diesel Production from Vegetable Oil. In *Sustainable Industrial Chemistry* (pp. 427–438). Weinheim, Germany: Wiley-VCH Verlag GmbH & Co. KGaA. doi:10.1002/9783527629114.ch8
- Chen, H., Wang, Q., Zhang, X., & Wang, L. (2014). Hydroconversion of Jatropha Oil to Alternative Fuel over Hierarchical ZSM-5. *Industrial & Engineering Chemistry Research*, 53(51), 19916–19924. doi:10.1021/ie503799t
- Chica, A., Strohmaier, K. G., & Iglesia, E. (2005). Effects of zeolite structure and aluminum content on thiophene adsorption, desorption, and surface reactions. *Applied Catalysis B: Environmental*, 60(3-4), 223–232. doi:10.1016/j.apcatb.2005.02.031
- Costa, C., Dzikh, I., Lopes, J. M., Lemos, F., & Ribeiro, F. R. (2000). Activity–acidity relationship in zeolite ZSM-5. Application of Brønsted-type equations. *Journal of Molecular Catalysis A: Chemical*, 154(1-2), 193–201. doi:10.1016/S1381-1169(99)00374-X
- Derouane, E. G., Védrine, J. C., Pinto, R. R., Borges, P. M., Costa, L., Lemos, M. A. N. D. A., Lemos, F., Ribeiro, F. R. (2013). The Acidity of Zeolites: Concepts, Measurements and Relation to Catalysis: A Review on Experimental and Theoretical Methods for the Study of Zeolite Acidity. *Catalysis Reviews*, 55(4), 454–515. doi:10.1080/01614940.2013.822266
- Hunger, B., Heuchel, M., Clark, L. a., & Snurr, R. Q. (2002). Characterization of acidic OH groups in zeolites of different types: An interpretation of NH₃-TPD results in the light of confinement effects. *Journal of Physical Chemistry B*, 106(15), 3882–3889. doi:10.1021/jp012688n
- Yusuf, C., (2013). Constraints to commercialization of algal fuels, *Journal of biotechn.*, 167(3), 201-14. doi: 10.1016/j.jbiotec.2013.07.020
- Miyamoto, Y., Katada, N., & Niwa, M. (2000). Acidity of β zeolite with different Si/Al₂ ratio as measured by temperature programmed desorption of ammonia. *Microporous and Mesoporous Materials*, 40, 271–281. doi:10.1016/S1387-1811(00)00264-X
- Niwa, M., & Katada, N. (1997). Measurements of acidic property of zeolites by temperature programmed desorption of ammonia. *Catalysis Surveys from Asia*, 1(2), 215–226. doi:10.1023/a:1019033115091
- Park, J.-Y., Park, M. S., Lee, Y.-C., Yang, J.-W. (2015). Advances in direct transesterification of algal oils from wet biomass, *Bioresource Techn.*, 184, 267-275. doi:10.1016/j.biortech.2014.10.089
- Peng, B., Yao, Y., Zhao, C., & Lercher, J. a. (2012). Towards Quantitative Conversion of Microalgae Oil to Diesel-Range Alkanes with Bifunctional Catalysts. *Angewandte Chemie*, 124(9), 2072–5. doi:10.1002/ange.201106243
- Pérez-Ramírez, J., Verboekend, D., Bonilla, A., & Abelló, S. (2009). Zeolite Catalysts with Tunable Hierarchy Factor by Pore-Growth Moderators. *Advanced Functional Materials*, 19(24), 3972–3979. doi:10.1002/adfm.200901394
- Souverijns, W., Martens, J. A., Froment, G. F., Jacobs, P. A. (1998). Hydrocracking of isoheptadecanes on Pt/H-ZSM-22: an example of pore mouth catalysis, *Journal of Catal.*, 174(2), 177-184. doi:10.1006/jcat.1998.1959
- van Laak, A. N. C., Zhang, L., Parvulescu, A. N., Bruijninx, P. C. A., Weckhuysen, B. M., de Jong, K. P., de Jongh, P. E. (2011). Alkaline treatment of template containing zeolites: Introducing mesoporosity while preserving acidity. *Catalysis Today*, 168(1), 48–56. doi:10.1016/j.cattod.2010.10.101
- Verboekend, D., & Pérez-Ramírez, J. (2011). Design of hierarchical zeolite catalysts by desilication. *Catalysis Science & Technology*, 1(6), 879. doi:10.1039/c1cy00150g
- Verma, D., Kumar, R., Rana, B. S., & Sinha, A. K. (2011). Aviation fuel production from lipids by a single-step route using hierarchical mesoporous zeolites. *Energy & Environmental Science*, 4(5), 1667. doi:10.1039/c0ee00744g
- Wang, W.-C., & Tao, L. (2016). Bio-jet fuel conversion technologies. *Renewable and Sustainable Energy Reviews*, 53, 801–822. doi:10.1016/j.rser.2015.09.016
- Zhao, C., Brueck, T., Lercher, J. A. (2013). Catalytic deoxygenation of microalgae oil to green hydrocarbons, *Green Chem.*, 15(7), 1720-1739. doi: 10.1039/C3GC40558C